Aligned Mats from Electrospun Single Fibers

Lisa S. Carnell,*,† Emilie J. Siochi,† Nancy M. Holloway,† Ralph M. Stephens,† Caroline Rhim,‡ Laura E. Niklason,§ and Robert L. Clark||

NASA Langley Research Center, Hampton, Virginia 23681; Department of Biomedical Engineering, Duke University, Durham, North Carolina 27708; Department of Biomedical Engineering, Yale University, New Haven, Connecticut 06520; and Department of Mechanical Engineering and Materials Science, Duke University, Durham, North Carolina 27708

Received May 1, 2008; Revised Manuscript Received May 1, 2008

ABSTRACT: Highly aligned electrospun micro- and nanoscale fibers and pseudowoven mats were produced via electrospinning by incorporating an auxiliary counter electrode to create an electric field of controlled geometry and magnitude. Two polymers were examined using this technique: a polyimide (CP2) and a biodegradable polymer, poly(glycolic acid) (PGA). Highly aligned electrospun CP2 fibers were on the order of 10 μm in diameter, and fiber spacing in the spun mats ranged between 25 and 30 μm. Electrospun PGA aligned fibers were on the order of 500 nm in diameter with spacing between fibers ranging from 7 to 10 μm in the spun mats. High-speed videography illustrated the influence of the auxiliary electrode on the elimination of jet whipping and bending instability commonly associated with the electrospinning process. The data presented here demonstrate the direct influence of an opposing electric field on the degree of fiber alignment and control of fiber placement.

Introduction

The electrospinning process was developed by Formhals[1] in 1934 and has been explored extensively in the past decade as an inexpensive and simple way to produce nonwoven fibers and mats for a variety of applications.[2–5] Although electrospinning is a relatively simple process, many variables affect fiber/mat quality, thus adding complexity to the method and making process optimization tedious. The basic factors affecting electrospun fiber properties include the polymer solution (conductivity, surface tension, viscosity, molecular weight, flow rate, and solvent−polymer interaction), distance between the collector and nozzle, design of the collector, and the applied voltage. These characteristics along with the synergistic interactions between the polymer solution parameters strongly influence the applied field required to create a fiber and affect the ability to fabricate nonwoven or aligned mats. Several investigators have studied the effects of these variables on the processing of microfibers, nanofibers, and mats.[6–10] While these areas are becoming widely understood, there remains a significant gap in the ability to control the fiber from jet initiation to collection.[11] The inability to predict fiber placement has been the limiting factor in producing aligned fibers and mats with controllable porosities. Several methods have been investigated to resolve this issue. Many researchers incorporated a rotating collector or drum to achieve fiber alignment.[12–14] The rotating drum approach generated fibers with good alignment; however, this technique offers neither control over fiber placement nor a high degree of alignment for individual fibers and mats. Several groups have produced highly aligned fibers using a wheel edge as the collector.[15,16] While this technique worked well at producing highly aligned fibers, it is limited by its capability to produce mats of usable size for many applications and offers little control in fiber spacing. The gap or gaplike method successfully employs two electrodes spaced apart to create highly aligned fibers[17–19] but has limitations in fiber placement and individual fiber alignment and is constrained by the requirement to collect material between two electrodes. An alternative method involves the use of dual collection rings, similar to the gap method, which uses rings rather than plates to collect the fibers.[20] Still other configurations include a multifield approach,[21] the use of patterned electrodes,[22,23] parallel electrodes,[23] gas flow assistance,[24] and innovative deposition techniques.[25,26] One of the more successful approaches has been the incorporation of a counter electrodes to aid in fiber alignment.[27–29] The counter electrode has demonstrated the best control over fiber alignment to date with several variations that produce differing results. The parallel grid using knife-edged aluminum bars helped to focus the electric field and control the fiber alignment much better than the parallel aluminum strips, as illustrated by Teo et al.[28] In this work, Teo et al. demonstrated that the electric field could be focused by positioning a knife edge blade at a 45° angle to the collector and adding a steel blade to the syringe needle to create a uniform electrostatic field. This setup produced excellent alignment; however, control over the bending instability of the electrospinning jet still presents a challenge. Teo and Ramakrishna[30] provide a comprehensive review of the current state of the electrospinning process and the vast array of techniques employed in an attempt to achieve aligned fibers. The objective of the work presented here is to demonstrate that applying a counter voltage with a negative electrode having similar geometries can influence fiber placement and alignment by controlling the shape and magnitude of the electric field, allowing controlled fabrication of highly aligned electrospun

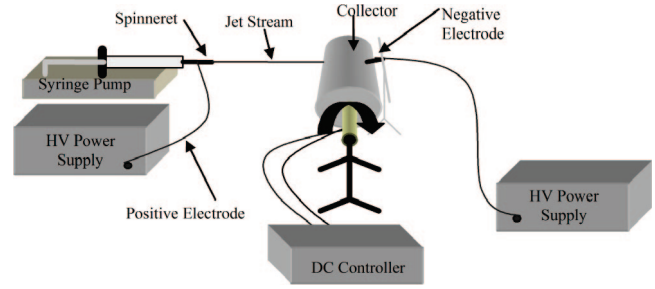

Figure 1. Electrospinning setup incorporating the auxiliary electrode configuration.

* To whom correspondence should be addressed: e-mail lisa.a.scottcarnell@nasa.gov; Tel (757) 864-4269; Fax (757)-864-8312.
† NASA Langley Research Center.
‡ Department of Biomedical Engineering, Duke University.
§ Yale University.
|| Department of Mechanical Engineering and Materials Science, Duke University.

10.1021/ma8000143 CCC: $40.75
Published on Web 06/26/2008

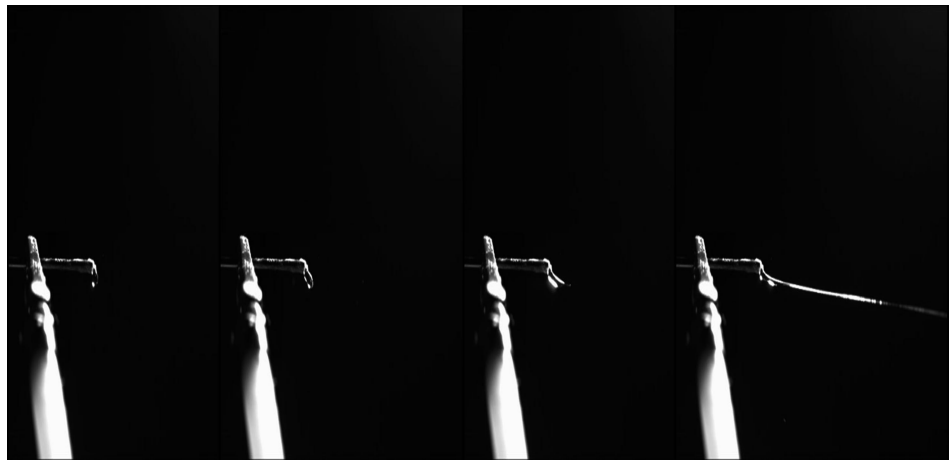

Figure 2. Jet exit with auxiliary electrode directly opposite the spinneret.

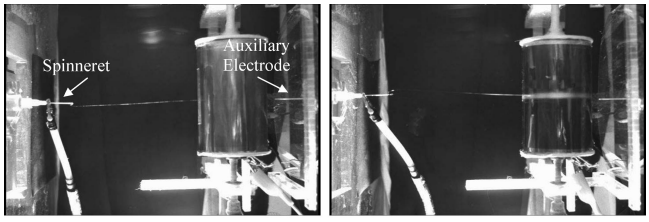

Figure 3. Jet stream collecting (a) as a straight fiber on the rotating mandrel and (b) after 5 min.

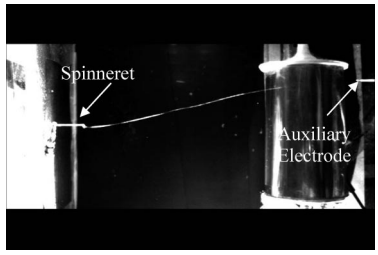

Figure 4. Jet stream with auxiliary electrode positioned offset of the spinneret.

fibers and mats. Unlike all documented literature on electrospinning thus far, this system design permits the virtual elimination of the bending instability typically associated with the electrospinning process.

Experimental Section

Materials. A colorless polyimide (CP2) developed by NASA Langley Research center ($[\eta] = 1.2$ dL/g) was obtained from SRS Technologies. Polyglycolic acid (PGA, $[\eta] = 1.12$ dL/g) was obtained from Durect Corp. (Pelham, AL). Chloroform and hexafluoroisopropanol (HFIP) were purchased from Fisher Scientific and E.I. du Pont de Nemours and Co., respectively. All materials were used as received. CP2 was dissolved in chloroform (10 wt %) at room temperature and allowed to stir for a minimum of 2 h prior to use. PGA was dissolved in HFIP under low heat and allowed to stir overnight until all particles were dissolved.

Electrospinning. CP2 was electrospun using a 10 mL syringe (Beckton Dickinson) and an 18 gauge blunt end needle (Small Parts, Inc.). A constant flow rate of 2 mL/h was obtained using a syringe pump (KD Scientific). A rotating collector (~2400 rpm) was positioned 13−17 cm from the tip of the needle. The collector was grounded, and polymer film was placed around the barrel of the collector to create an insulative surface. An alligator clip was used to attach the high-voltage power supply (Spellman CZE 1000R) to the needle to distribute a positive voltage of 10 kV to the polymer solution. PGA was electrospun using a 10 mL syringe and a 22 gauge blunt end needle at a constant flow rate of 1.5 mL/h. The rotating collector was positioned 10−17 cm from the tip of the needle, and a positive voltage of 15 kV was applied to the polymer solution. For each polymer, an auxiliary electrode (stainless steel needle) was positioned at an angle 90° directly above the top of the rotating collector using a Plexiglas mounting bracket. An alligator clip was used to attach the high-voltage power supply (Acopian Technical Company) to the auxiliary electrode to generate a negative voltage equal and opposite to the positive voltage.

Characterization. Fibers and mats were coated with 4−8 nm of Au/Pd using a Hummer VI sputter coater (Anatech, Inc.). Images were obtained using a JEOL JSM 5600 scanning electron microscope and a Phillips XL30 high-resolution scanning electron microscope. Image processing and analysis of fiber diameter and degree of alignment were performed with Image J (http://rsb.info.nih.gov/ij/).

High-Speed Video Imaging. High-speed videos were captured at 2000 frames/s using a Phantom Model 7 camera (Vision Research, Inc.). Data were processed using Phantom software (Vision Research, Inc.) and postprocessed using Adobe Premiere Elements (Adobe Systems, Inc.).

Results and Discussion

Electrospinning is typically performed with a grounded collector such as a static plate, wire mesh, or a rotating drum fabricated from a variety of shapes and configurations. The collector is generally made from aluminum or copper, as most nonconductive surfaces do not draw the jet stream to the collector readily. In this experiment an auxiliary electrode was incorporated, as illustrated in Figure 1, in an attempt to control the placement and alignment of the fibers based on electric field theory which states that a positive field being emitted will be attracted to a negative field. In this setup, similar geometries were employed for the electrode and the counter electrode to create a uniform spherical electric field. On the basis of this principle, it should follow that the polymer jet would track the electric field lines and attempt to attach to the negatively charged auxiliary electrode. The rotating collector would intercept the fibers prior to their reaching the auxiliary electrode, gathering aligned fibers with fairly uniform spacing. High-speed video imaging was used to capture the fiber from jet initiation through collection on the rotating mandrel. Jet exit images (Figure 2) illustrate the stability of the fiber as it overcomes surface tension and is drawn into the electric field. The fiber continues along the field line path and is pulled straight to the rotating mandrel (Figure 3a) when an auxiliary counter

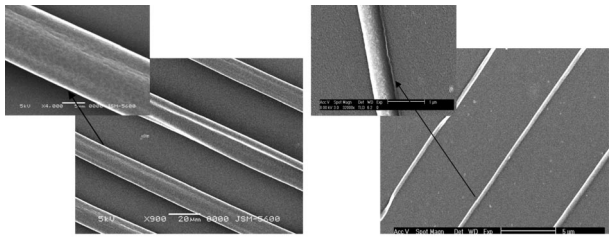

(a) (b)

Figure 5. Electrospun fibers from (a) CP2 having an average diameter of 10 μm and 25−30 μm spacing and (b) PGA having an average diameter of 500 nm and 7−10 μm spacing.

electrode is present to focus the field. Jet whipping and bending instability that are typical characteristics of electrospinning were not observed as shown in Figures 2 and 3. The fiber continues to follow the straight electric field path after a period of 5 min as depicted in Figure 3b. In order to verify the influence of the auxiliary counter electrode on controlling fiber placement and alignment, the location of the auxiliary counter electrode was repositioned to a location offset from the spinneret. As illustrated in Figure 4, the fiber is directed to the rotating mandrel only at the location of auxiliary counter electrode.

In order to determine the effect of the electric field on the fiber alignment and distribution over time, each polymer was collected for a period of 30 s. Fibers that were electrospun from CP2 were on the order of 10 μm in diameter (Figure 5a). The spacing between fibers was fairly uniform and ranged from approximately 25 to 30 μm. Nanofibers were observed for the PGA polymer as illustrated in the micrographs shown in Figure 5b. The PGA fibers were approximately 500 nm−1 μm in diameter with spacing between fibers in the range of 7−10 μm. The uniform spacing may be attributed to a combination of two factors: the positive charge present on the fibers causing them to repel each other[16] and the uniform shape of the electric field due to the similar geometries employed for the electrodes.

Pseudowoven mats were generated by electrospinning multiple layers in a 0°/90° layup. This was achieved by electrospinning the first layer onto a polymer film attached to the collector, removing the polymer film, rotating it 90°, reattaching it to the collector, and electrospinning the second layer on top of the first, resulting in the second layer lying 90° relative to the first layer. Fibers were collected for 1 min in each direction. A high degree of alignment was observed in this configuration as shown in the SEM micrographs (Figure 6a,b). In order to assess the quality of a thicker pseudowoven mat, the layup procedure was repeated 15 times in each direction (0°/90°) for a period of 30−60 s for each orientation, generating a total of 30 layers as illustrated in Figure 7. The average fiber diameter for the CP2 pseudowoven mat was 9.9 ± 3.3 μm, and the PGA mat had an average fiber diameter of 0.91 ± 0.4 μm. The distribution in fiber diameter is illustrated in the histograms shown in Figure 8. PGA exhibited a much narrower Gaussian fiber diameter distribution while the CP2 polymer had a much broader range of fiber diameters. The degree of alignment was determined for each material by measuring the angle of the long axis of the fiber relative to the plane of the collector at deposition for each 0°/90° orientation. The data obtained for both polymers indicated excellent alignment with CP2 having an average degree of alignment of 89.7 ± 1.7° and PGA with 89.5 ± 4.8°. The control of fiber placement and alignment shown in parts a and b of Figure 7 for CP2 and PGA, respectively, demonstrate that it is possible to fabricate pseudowoven mats of varying thickness depending on the application requirements.

Skewing of some fibers on the top layer of the thick PGA mat (Figure 7b) was primarily caused by the physical shifting of the nanofibers when the mat was being removed from the collector to prepare it for imaging in the SEM. Manually rotating the polymer collector film may have contributed to minor degrees of unaligned fibers as well, although this procedure produced excellent pseudowoven mats with a high degree of alignment.

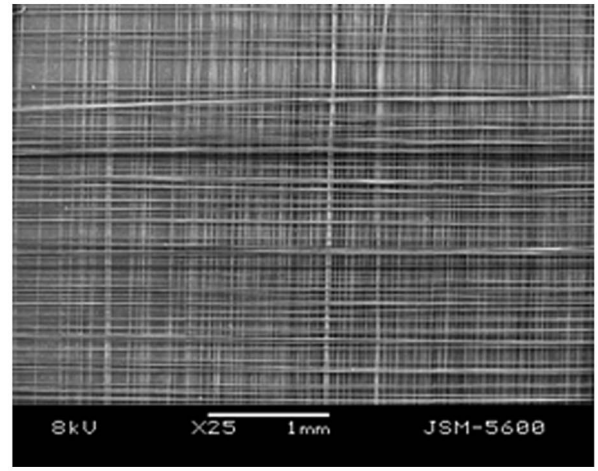

(a)

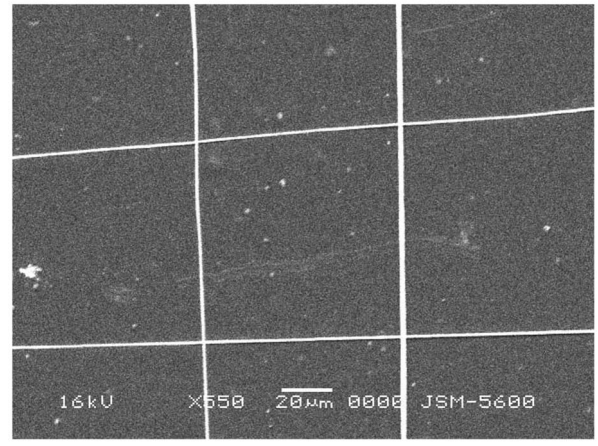

(b)

Figure 6. Electrospun mats with a single layer 0°/90° layup from (a) CP2 (magnification 25×) and (b) PGA (magnification 500×).

Conclusions

Highly aligned electrospun fibers and pseudowoven mats were produced using a new technique where an auxiliary electrode permitted tailoring of the electric field to direct the position of the polymer jet. High-speed videography confirmed the elimination of jet whipping and bending instability commonly associated with the electrospinning process. The process was demonstrated on two different classes of polymers: nonbiodegradable CP2 polyimide and biodegradable PGA. Both materials were successfully electrospun into aligned pseudowoven mats with reasonably controlled porosity. This study demonstrates substantial improvement of fiber placement and alignment on both the microscale and nanoscale through the use of an auxiliary electrode regardless of the polymer selected. The results suggest that controlling the shape and magnitude of the electric field influences fiber deposition and alignment, thus allowing mat porosity to be tailored to specific applications.

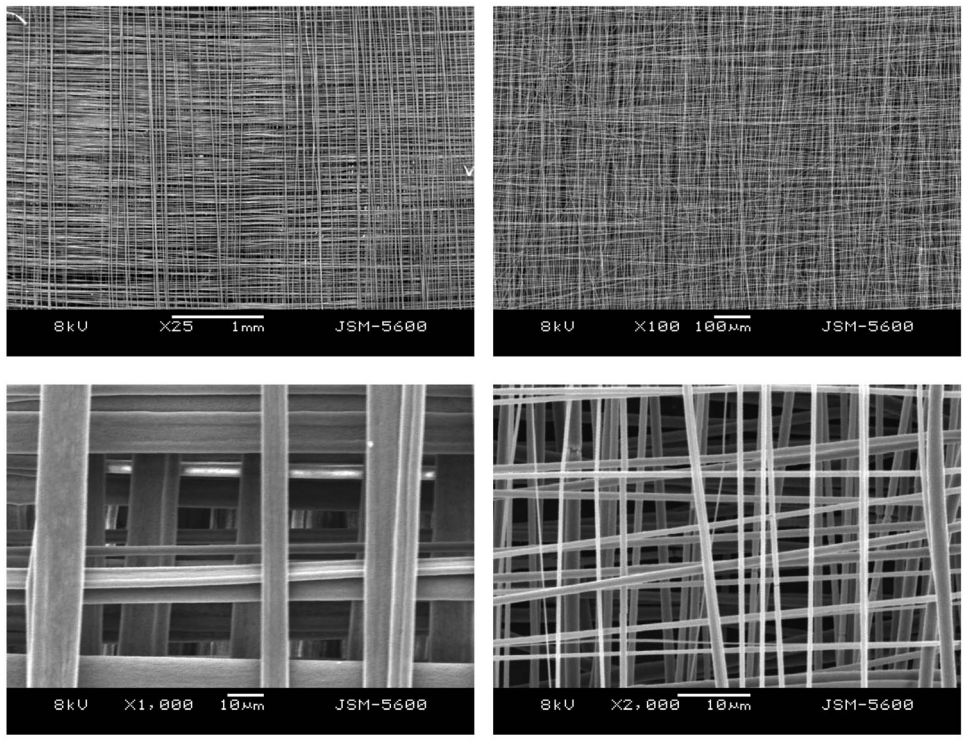

(a) (b)

Figure 7. Electrospun pseudowoven mats with 30 layers alternating 0°/90° layup. (a) CP2: top image magnification 25×; bottom image magnification 1000× (average degree of alignment 89.7 ± 1.7°). (b) PGA: top image magnification 100×; bottom image magnification 2000× (average degree of alignment 89.5 ± 4.8°).

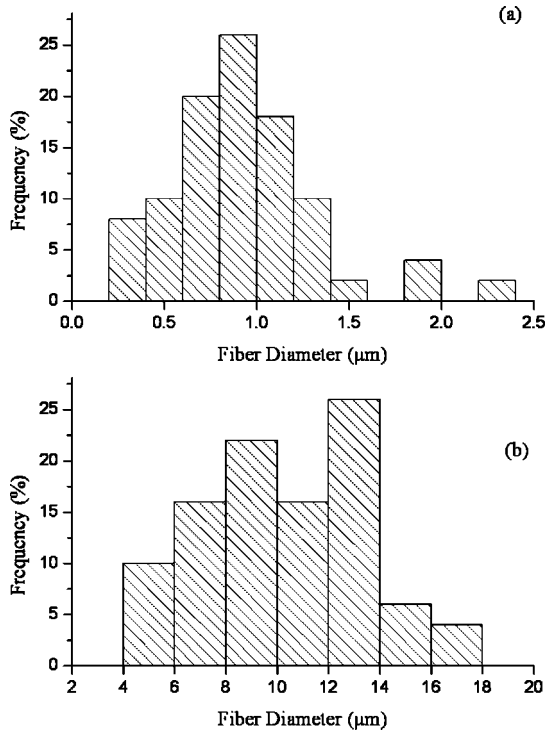

Figure 8. Fiber diameter distribution for (a) PGA (average 0.91 ± 0.4 μm) and (b) CP2 (average 9.9 ± 3.3 μm).

Acknowledgment. This work was supported by NASA Langley Research Center under Grant NGT-1-03008. We thank Pete Lillehei for his assistance and valuable discussions pertaining to SEM imaging and Paul Bagby for videography support.

Supporting Information Available: A short video clip illustrating elimination of the jet whipping and bending instability. This material is available free of charge via the Internet at http://pubs.acs.org.

References and Notes

(1) Formhals, US Patent 1,975,504, **1934**.
(2) Dersch, R.; Liu, T. Q.; Schaper, A. K.; Greiner, A.; Wendorff, J. H. *J. Polym. Sci., Part A: Polym. Chem.* **2003**, *41*, 545–553.
(3) Reneker, D. H.; Chun, I. *Nanotechnology* **1996**, *7*, 216–223.
(4) Tan, S. H.; Inai, R.; Kotaki, M.; Ramakrishna, S. *Polymer* **2005**, *46*, 6128–6134.
(5) Huang, Z. M.; Zhang, Y. Z.; Kotaki, M.; Ramakrishna, S. *Compos. Sci. Technol.* **2003**, *63*, 2223–2253.
(6) Deitzel, J. M.; Kleinmeyer, J.; Harris, D.; Tan, N. C. B. *Polymer* **2001**, *42*, 261–272.
(7) Theron, S. A.; Zussman, E.; Yarin, A. L. *Polymer* **2004**, *45*, 2017–2030.
(8) Fridrikh, S. V.; Yu, J. H.; Brenner, M. P.; Rutledge, G. C. *Phys. Rev. Lett.* **2003**, *90*, 144502.
(9) He, T. H.; Wan, Y. Q.; Yu, J. Y. *Polymer* **2005**, *46*, 2799–2801.
(10) Shin, Y. M.; Hohman, M. M.; Brenner, M. P.; Rutledge, G. C. *Polymer* **2001**, *42*, 9955–9967.
(11) Dzenis, Y. *Science* **2004**, *304*, 1917–1919.
(12) Fennessey, S. F.; Farris, R. J. *Polymer* **2004**, *45*, 4217–4225.
(13) Katta, P.; Alessandro, M.; Ramsier, R. D.; Chase, G. G. *Nano Lett.* **2004**, *4*, 2215–2218.
(14) Sundaray, B.; Subramanian, V.; Natarajan, T. S.; Xiang, R. Z.; Chang, C. C.; Fann, W. S. *Appl. Phys. Lett.* **2004**, *84*, 1222–1224.
(15) Xu, C. Y.; Inai, R.; Kotaki, M.; Ramakrishna, S. *Biomaterials* **2004**, *25*, 877–886.
(16) Yang, F.; Murugan, R.; Wang, S.; Ramakrishna, S. *Biomaterials* **2005**, *26*, 2603–2610.
(17) Li, D.; Wang, Y. L.; Xia, Y. N. *Adv. Mater.* **2004**, *16*, 361–366.
(18) Teo, W. E.; Ramakrishna, S. *Nanotechnology* **2005**, *16*, 1878–1884.
(19) Kakade, M. V.; Givens, S.; Gardner, K.; Lee, K. H.; Chase, D. B.; Rabolt, J. F. *J. Am. Chem. Soc.* **2007**, *129*, 2777–2782.
(20) Dalton, P. D.; Klee, D.; Moller, M. *Polymer* **2005**, *46*, 611–614.
(21) Deitzel, J. M.; Kleinmeyer, J. D.; Hirvonen, J. K.; Tan, N. C. B. *Polymer* **2001**, *42*, 8163–8170.

(22) Li, D.; Ouyang, G.; McCann, J. T.; Xia, Y. N. *Nano Lett.* **2005**, *5*, 913–916.
(23) Kim, G.; Kim, W. *Appl. Phys. Lett.* **2006**, *88*, 233101.
(24) Zhou, W. P.; Li, Z. F.; Zhang, D.; Liu, Y. P.; Wei, F.; Luo, G. H. *J. Nanosci. Nanotechnol.* **2007**, *7*, 2667–2673.
(25) Kameoka, J.; Craighead, H. G. *Appl. Phys. Lett.* **2003**, *83*, 371–373.
(26) Bellan, L. M.; Craighead, H. G. *J. Vac. Sci. Technol. B* **2006**, *24*, 3179–3183.
(27) Mo, X. M.; Weber, H. J. *Macromol. Symp.* **2004**, *217*, 413–416.
(28) Teo, W. E.; Kotaki, M.; Mo, X. M.; Ramakrishna, S. *Nanotechnology* **2005**, *16*, 918–924.
(29) Pan, H.; Li, L. M.; Hu, L.; Cui, X. J. *Polymer* **2006**, *47*, 4901–4904.
(30) Teo, W. E.; Ramakrishna, S. *Nanotechnology* **2006**, *17*, R89–R106.

MA8000143